Journal of Analytical and Applied Pyrolysis 110 (2014) 147–154

Contents lists available at ScienceDirect

Journal of Analytical and Applied Pyrolysis

journal homepage: www.elsevier.com/locate/jaap

Detailed characterization of red oak-derived pyrolysis oil: Integrated use of GC, HPLC, IC, GPC and Karl-Fischer

Yong S. Choi[a], Patrick A. Johnston[b], Robert C. Brown[b], Brent H. Shanks[a,**], Kyong-Hwan Lee[c,*]

[a] Department of Chemical and Biological Engineering, Iowa State University, Ames, IA 50011, USA
[b] Center for Sustainable Environmental Technologies, Iowa State University, Ames, IA 50011, USA
[c] Climate Change Research Division, Korea Institute of Energy Research, 102 Gajeong-ro, Yuseong-gu, Daejeon 305-343, Korea

ARTICLE INFO

Article history:
Received 19 June 2014
Accepted 24 August 2014
Available online 17 September 2014

Keywords:
Bio-oil
Characterization
Analytical techniques
Quantification
Reproducibility

ABSTRACT

Red oak bio-oil obtained from fast pyrolysis in a fluidized bed reactor was fully analyzed using gas chromatography/mass spectrometry (GC/MS), high-performance liquid chromatography (HPLC), ion chromatography (IC), gel permeation chromatography (GPC) and Karl-Fischer titration. Based on the chemical speciation, we achieved a high mass balance closure of bio-oil (92 wt%). Of the analytical techniques, GC accounted for the largest portion of the bio-oil (25.7 wt%), followed by HPLC (15.4 wt%) and IC (8.1 wt%). Monosaccharides and disaccharides (not detected by GC) were characterized by HPLC, and total sugars present in bio-oil were estimated by running acid-hydrolysable sugars in the HPLC. Quantity of pyrolytic lignin, oligomer of lignin-derived phenolic compounds, was determined as a GC-undetected portion of water-insolubles of a whole bio-oil. Small standard deviation of each compound between duplicate runs indicated a reproducibility of pyrolysis experiments and bio-oil characterizations validating the detailed analytical approach used.

1. Introduction

Interest in liquid biofuels has grown due to the depletion of fossil resources, increasing energy demand, and concerns over global warming. Although ethanol, produced by a biochemical conversion of sugarcane and grain, has been commercially available, there has been a debate over "food vs. fuel" owing to its usage of edible crop feedstocks. Therefore, significant incentive exists to use non-edible crops to produce biofuels. Advanced biofuels, manufactured from non-edible cellulosic biomass, are receiving significant attention with fast pyrolysis being considered as one of the more promising technologies for economically producing advanced fuels. Fast pyrolysis is defined as rapid thermal degradation of biomass in the absence of oxygen, in order to produce a bio-oil as the primary product along with char and gases [1]. High heating rates, short vapor residence times, and rapid cooling of vapors are generally required to maximize bio-oil yield during fast pyrolysis [1,2]. In general, bio-oil is a complex mixture of more than 300 oxygenated organic compounds [3,4] and can be broadly classified into anhydrosugars, phenolics, furan/pyran derivatives, and C2–C4 low-molecular-weight compounds. Due to number of organic compounds generated, bio-oil has the potential to be upgraded into transportation fuels and commodity chemicals via catalytic conversion [1,5–7].

To design and develop robust downstream process strategies for upgrading bio-oil, it is necessary to know its full chemical properties but given its complexity a detailed chemical speciation of bio-oil has been elusive. While as many of the plethora of species in bio-oil are reported in literature, typically only compounds of interest among the identified compounds have been quantified [3,8,9]. Additionally, most of the chemical analyses of bio-oil were performed using GC which is limited to detection of volatile compounds. For example, only 30–35 wt% of the total bio-oil was determined by quantification of 30–40 compounds using GC [8,9]. Di Blasi and coworkers [10] characterized bio-oil from low-temperature pyrolysis of wood using GC-MS, with an identification of 90 species and a quantification of 40 species, addressing 43 wt% of the bio-oil. Mullen et al. [3] used both GC and HPLC for chemical analyses of bio-oil derived from switchgrass and alfalfa, which accounted for 9–18 wt% of the bio-oil by quantification of 24 compounds out of 56 identified compounds. Due to these incomplete characterizations, bio-oil analysis studies in literature have

* Corresponding author. Tel.: +82 42 860 3774.
** Corresponding author. Tel.: +1 515 294 1895.
E-mail addresses: bshanks@iastate.edu (B.H. Shanks), khwanlee@kier.re.kr (K.-H. Lee).

http://dx.doi.org/10.1016/j.jaap.2014.08.016
0165-2370/

Table 1
Ultimate and proximate analyses of the red oak feedstock (wt%).

Ultimate analysis		Proximate analysis	
Carbon	45.8	Moisture	8.3
Hydrogen	6.7	Volatiles	78.6
Nitrogen	0.1	Fixed carbon	12.7
Oxygen	47.4	Ash	0.3
Total	100	Total	99.9
HHV, MJ/kg	17.6		

HHV = $\{33.5[C] + 142.3[H] - 15.4[O] - 14.5[N]\} \times 10^{-2}$ [21].

not attempted to perform detailed overall mass balance closure for the bio-oils. In the current study, an integrated characterization strategy was to determine the detailed chemical compositions of bio-oil obtained from fast pyrolysis of red oak. Included in the studies were analyses conducted using GC, HPLC, IC, elemental analysis, and Karl-Fischer titration.

2. Experimental

Duplicate runs of red oak fast pyrolysis were conducted in a fluidized bed reactor and the collected bio-oil from the runs was fully analyzed using a variety of analytical instruments as discussed below.

2.1. Materials

Red oak, ground and sieved to 250–500 μm particles, was used as the feedstock for the pyrolysis experiments. As shown in Table 1, ultimate and proximate analysis of the feedstock was performed. The fluidizing medium used in the reactor was silica sand with an average particle size of 512 μm (provided by Badger Mining Corporation) as this size provided good fluidization in the bed for the carrier gas flow rate (10 L/min).

2.2. Pyrolysis experiments

2.2.1. Pyrolysis in the fluidized bed reactor

A bench-scale bubbling fluidized bed reactor with a feed rate of 100 g/h, shown in Fig. 1, was used in this study. Nitrogen was used to fluidize the inert silica sand bed during pyrolysis. The fluidized bed reactor system was primarily composed of a screw feeder, fluidized-bed reactor, and series of condensers. Sufficient amount of feedstock was placed in the hopper prior to supply the entire run, with the feedstock introduced to the reactor through an injection auger. The auger was calibrated to deliver 100 g/h of feedstock to the reactor. The reactor was made of from a standard 316 stainless steel pipe with a 38.1 mm inner diameter and height of 0.34 m. The plenum region was located at the bottom of the reactor, which was designed to preheat the nitrogen carrier gas. The reactor and plenum were encased with a heater and

Table 2
Process parameters used for the fluidized bed pyrolysis.

Residence time (s)	Sand size (μm)	N_2 flow rate (L/min)	U/U_{mf}	d_{eq}/D
1.3	512	10.0	2.8	65.3

U, superficial velocity at given N_2 flow rate at 500 °C; U_{mf}, minimum fluidization velocity; d_{eq}, volume-equivalent diameter of bubble; D, bed diameter.

maintained at 500 °C through a process control loop. Solid particles generated during pyrolysis were collected downstream of the reactor in a series of cyclones. Hot vapors exiting the reactor and cyclones were subjected to a cold quench of liquid nitrogen in which the vapors were quenched at 90 °C. Then, the cooled vapors were passed through an electrostatic precipitator (ESP) to remove aerosols and heavy molecules. Following the ESP, the vapors were passed through a heat exchanger maintained at −10 °C and collected in two stages. Non-condensable gases leaving the condenser system were passed through a wet test meter to measure their total volumetric flow rate. The concentrations of these gases were measured using an online micro-GC-TCD (Varian CP 4900) equipped with three columns for different gases: Varian® Molesieve 5A column for H_2, N_2, CH_4, and CO, Varian® PoraPLOT Q column for CO_2, C_2H_2, C_2H_4, and C_2H_6, and Varian® Al_2O_3 column for C_3H_8. After the reaction, the bio-oil yield was calculated by considering the sum of the bio-oil fractions. The total char amount included solid particles collected in the cyclones as well as in the reactor (minus the silica). The pyrolysis runs were duplicated to evaluate the reproducibility of the experimental data.

2.2.2. Bed fluidization

To ensure the bed fluidization conditions created a high heat transfer rate, values of U/U_{mf} and d_{eq}/D for the 10 L/min of carrier gas rate were set between 2 and 3 and below 70%, respectively [11], by appropriate selection of the sand particle size. U is the superficial velocity at the given flow rate at 500 °C, U_{mf} is the minimum velocity for fluidization, i_{eq} is a volume-equivalent diameter of a bubble, and D is the bed diameter. Table 2 shows the process parameters used for the fluidized bed runs.

2.2.3. Separation of whole bio-oil into water-soluble and water-insoluble fractions

Immediately after a pyrolysis reaction run, the bio-oil fractions collected during the continuous reaction were mixed for 12 h with this mixture denoted as the whole bio-oil. The bio-oil was then separated into a water-soluble fraction and water-insoluble fraction by adding distilled water with mixing to the whole bio-oil at a ratio of 1.7 wt water/wt whole bio-oil. The sample was exposed to vortex mixing for 40 min followed by centrifugation at 3500 rpm for 10 min at which point a phase separation of the water-solubles and water-insolubles occurred. The water-soluble fraction was

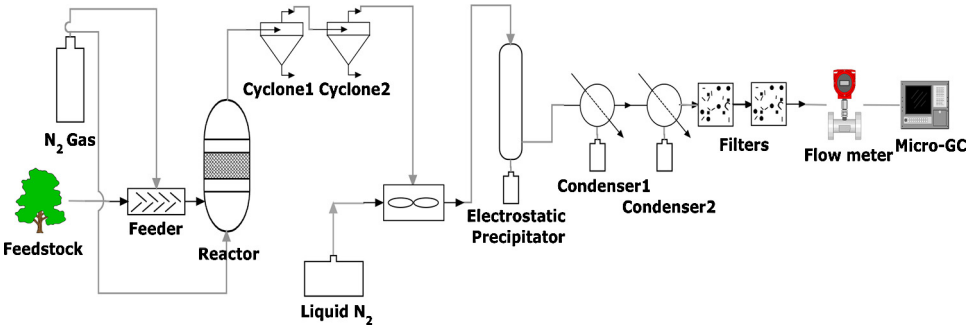

Fig. 1. Schematic diagram of the fluidized bed reactor system.

collected by decanting the liquid phase from the water-insoluble fraction. The three sets of bio-oil samples (whole bio-oil, water-soluble fraction, and water-insoluble fraction) were individually analyzed for use in the overall mass balance.

2.3. Bio-oil characterization

There is no single analytical technique that can be used to perform a complete analysis of bio-oil, due to its complex mixture of organic compounds. Thus, a range of analytical methods were employed in the current study to elucidate and quantify as many species in the bio-oil as possible. The full analysis of the bio-oils was conducted using GC, HPLC, IC, elemental analysis, and Karl-Fischer titration. GC was used for volatile compounds; HPLC for semi- or non-volatile saccharides; IC for thermally labile organic acids; and Karl-Fischer for water content. To minimize aging effects during the characterization period, all bio-oil samples were stored in tightly sealed Nalgene® bottle at 4 °C and all of the chemical analyses of the samples were conducted within 2 weeks of their production.

2.3.1. Gas chromatography

A GC-MS/FID was used to characterize the volatile compounds in the bio-oil with the mass spectrometer (MS) for identification and the flame ionization detector (FID) for quantification. The column used for chromatographic separation was a Zebron ZB-1701 coated with 14% cyanopropylphenyl and 86% dimethylpolysiloxane with dimensions of (60 m × 0.25 mm ID × 0.25 μm film thickness). The GC oven was programmed to hold at 35 °C for 3 min, ramp at 5 °C/min to 300 °C, and then hold for 4 min. The injector was maintained at 300 °C and employed a split ratio of 30:1. The flow rate was 1 mL/min of the helium carrier gas. The mass spectrometer was configured for electron impact ionization, with a source/interface temperature of 280 °C. The mass-to-charge ratio (m/z) values of the compound fragment ions were recorded for each species exiting the GC column. Full scan mass spectra were acquired from a 35 to 650 m/z at a scan rate of 0.5 s per scan. The peak assignment to a compound was conducted using a NIST mass spectra library search in conjunction with the literature [12–16]. The assignments were confirmed by injection of a pure standard into the GC.

To quantify each of the identified compounds, four known concentrations of each pure component, diluted with methanol and phenanthrene (internal standard), were injected into the GC-FID. The peak areas of each component and the internal standard were then integrated and the relative areas were used to produce a calibration curve. The calibration curves for the pure compounds all had strong linear relationships ($R^2 \geq 0.90$) between the FID response and concentration of the standard. For the calibrated cyclic compounds, a relationship ($R^2 = 0.85$) between the ratio of total molecular weight to carbon weight (MW_{total}/MW_{carbon}) and the FID relative response factor was established (Fig. 2) [17]. This correlation was used to approximate the FID relative response for the cyclic compounds, which were unavailable commercially. The compounds, which used the estimated FID response factor included, 2-hydroxy-3-oxobutanal, 2-methyl-2-cyclopenten-1-one, 2-hydroxy-2-cyclopenten-1-one, 3-methyl-2-cylcopenten-1-one, 4-hydroxy-5,6-dihydro-(2*H*)-pyran-2-one, 4-ethyl-2,6-dimthoxyphenol, 2,6-dimethoxy-4-vinylphenol, and 2,6-dimethoxy-4-(1-propenyl)phenol. Peak assignment to the unavailable compound was determined by comparing fragmentation patterns of the unknown peaks with those reported in the literature [12–16].

Three bio-oil samples, whole bio-oil, water-soluble fraction, and water-insoluble fraction, were individually prepared at approximately 15 wt% in a solution of methanol/acetone and phenanthrene. The diluted sample was filtered through a Whatman® 0.45 micron glass microfiber filter with1 μL injected into the GC.

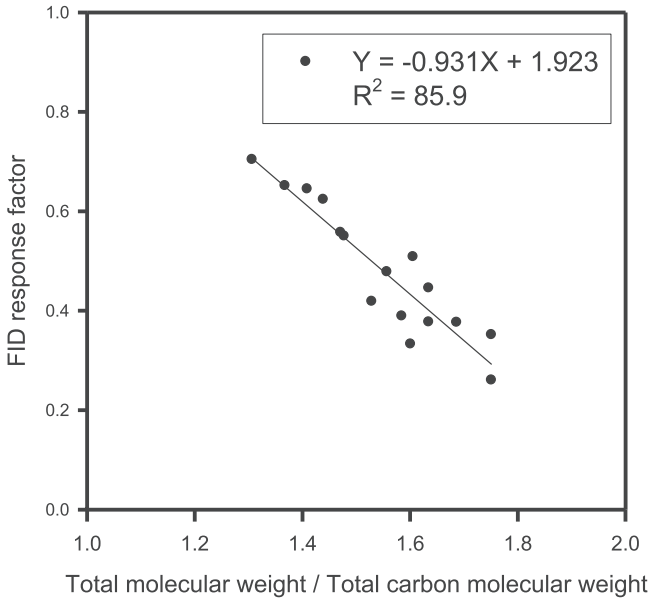

Fig. 2. Correlation between MW_{total}/MW_{carbon} and FID response to approximate response factors of commercially unavailable cyclic compounds.

2.3.1.1. Quantification of pyrolytic lignin. Although bio-oil water extraction method is widely used to separate and quantify pyrolytic lignin in bio-oil [18], the amount of pyrolytic lignin in this study was determined as an undetected portion (by GC) of the water-insolubles. It is expected that the pyrolytic lignin measurement in this study was more accurate than the method reported in the literature, since the water-insolubles that were considered as pyrolytic lignin in the prior method may contain monomeric phenols, sugars, and low-molecular-weight compounds (LMWs), which can be detected by GC. The non-GC detectables in the water-insoluble fraction were used with the appropriate ratio for the mass balance for the whole bio-oil.

2.3.2. High-performance liquid chromatography

2.3.2.1. Water-soluble sugars. A HPLC equipped with a refractive index (RI) detector was used to characterize the non/semi-volatile sugars that can be dissolved in water such as levoglucosan, cellobiosan, xylose, and maltosan. The columns used were two Bio-Rad Aminex HPX-87P with a guard column. The column temperature was 75 °C with a flow rate of 0.6 mL/min 18.2 Ω distilled water. The RI detector was calibrated with the non-volatile sugars diluted into five concentrations (0–10 mg/ml) with distilled water. Calibration standards were obtained from Carbosynth (levoglucosan, cellobiosan, and maltosan) and Thermo Fisher Scientific (xylose). Approximately 0.5 g of a bio-oil sample was dissolved in 5 ml of distilled water and well mixed with a vortex mixer for 20 min. The resulting solution was then filtered through a Whatman® 0.45 micron glass microfiber filter and 25 μL were injected into the HPLC.

2.3.2.2. Total sugars. Hydrolysable sugars in bio-oil were quantified by HPLC with a Shodex refractive index detector to estimate total sugar amount in the bio-oil. Under dilute acid condition, oligosaccharides were hydrolyzed into monosaccharides by the breaking of glycosidic bonds [19,20], and the monosaccharides were further converted into glucose or sorbitol (for C6 sugars) and xylose (for C5 sugars). Sugars in the bio-oil were detected in the form of glucose, sorbitol, or xylose by the HPLC system and the

detected monosaccharide amount was used to approximate the total sugars in the bio-oil. The column used was a HyperRez XP Carbohydrate (300 mm × 7.7 mm × 8 μm particle size). The mobile phase was 18.2 Ω deionized water with a flow rate of 0.2 mL/min and the column was set at 55 °C. Approximately 60 mg of bio-oil and 6 mL of 400 mM H_2SO_4 were added to a sealed glass vial, and the sugars were acid-hydrolyzed in an oil bath at conditions of 125 °C for 60 min. The hydrolyzed solution was then filtered through a Whatman® 0.45 micron glass microfiber filter, and 25 μL were injected into the HPLC.

2.3.3. Ion chromatography

Carboxylic acids including acetic acid, formic acid, glycolic acid, and propanoic acid were characterized by IC as their broad peak shapes lead to inaccurate quantification by GC-FID [9]. The IC system used was a Dionex ICS3000 equipped with a conductivity detector and an Anion Micromembrane Suppressor AMMS-ICE 300. The suppressor regenerant was 5 mM tetrabutylammonia hydroxide at a flow rate of 4–5 mL/min. The mobile phase was 1.0 mM heptaflourobutyric acid used in an IonPac® ICE-AS1 analytical column at a flow rate of 0.120 mL/min at 19 °C. The conductivity detector was calibrated with a standard solution (purchased from Inorganic Ventures) containing the four acids diluted into five concentrations (10–200 mg/L). Peak assignment was determined by comparing peak retention times of the standard to those in the bio-oil sample. The bio-oil samples were prepared using 6 mL distilled water and 1.5 mL of methanol. The diluted samples were filtered with a syringe filter (0.45 μm) prior to injection.

2.3.4. Elemental analysis

Ultimate analysis of the biomass and bio-oil samples was conducted using an Elementar® elemental analyzer (vario MICRO cube). During elemental analysis, a sample was combusted at 900 °C, and the combustion products, carbon dioxide, water and nitric oxide, were characterized by a TCD. The weight percentages of C, H and N were calculated based on the amount of the combustion products. Oxygen was calculated by difference. Approximately 5 mg of sample was weighed and inserted into the combustion chamber for the analysis.

2.3.5. Thermogravimetric analysis

Proximate analysis of the feedstock was performed in a TGA with the following method: approximately 20 mg of biomass was heated in 100 mL/min of N_2 from 25 to 105 °C at 10 °C/min and held at 105 °C for 40 min to eliminate moisture in the biomass. The temperature was further increased to 900 °C at 10 °C/min and held for 20 min to quantify the volatiles. Then, 100 mL/min of air was introduced at 900 °C for 30 min to combust the remainder of the sample, with the subsequent weight loss being considered fixed carbon. The amount of ash was determined by the residual weight of the sample.

2.3.6. Karl-Fischer titration

The water content of the bio-oil was determined by Karl-Fischer titration (titrator).

2.3.7. Gel permeation chromatography

GPC is a type of size exclusion chromatography where the separation occurs on the basis of the size of the analytes. Small analytes elute slower than large analytes, since small molecules are retained longer in the pores of the stationary phase of the column. GPC analysis was performed on a HPLC system (Dionex Ultimate 3000) equipped with a Shodex Refractive Index (RI) and Diode Array Detector (DAD) detector. Two Agilent PLgel 3 μm × 100 Å, 300 mm × 7.5 mm columns and one Mesopore 300 mm × 7.5 mm analytical column were used. The mobile phase (tetrahydrofuran, THF) flowed into the column at a rate of 1.0 mL/min at 25 °C. Seven polystyrene standards with peak molecular weights of 162, 380, 580, 970, 1930, 2900, and 3790 were used for molecular weight calibration. A 0.02 g bio-oil sample was dissolved in a 10 mL of THF, with the solution filtered using a syringe filter (0.45 μm) prior to the GPC analysis. Data were acquired and evaluated using Dionex Chromeleon software, Version 6.8.

Table 3
Compositional analysis of the red oak feedstock.

Component	Composition (wt%)
Cellulose	40.7
Hemicellulose	22.8
Lignin	33.3
Ash	0.4
Total	97.2

Conducted by the protocol of the NREL Chemical Analysis and Testing Standard Procedures: NREL LAP, TP-510-42618.

3. Results and discussions

3.1. Biomass properties

According to composition analysis of red oak reported in Table 3, it is composed of 40.7 wt% cellulose, 22.8 wt% hemicellulose, and 33.3 wt% lignin, indicating that approximately two-thirds of the feedstock is hollocellulose. Proximate and ultimate analyses of the as-received red oak feedstock are given in Table 1. According to the proximate analysis, the feedstock had 8.3 wt% moisture, which is in the typical range. Based on the elemental analysis, higher heating value (HHV, MJ/kg) of red oak was calculated by the following formula, HHV = $\{33.5[C] + 142.3[H] - 15.4[O] - 14.5[N]\} \times 10^{-2}$ [21]. Carbon, hydrogen, and nitrogen were determined in the whole bio-oil and are shown in Table 4. The oxygen content was calculated by difference. The elemental analysis of the bio-oil yielded an average chemical formula of $C_{2.2}H_{2.3}O$, which corresponded to approximately 35 wt% oxygen (compared to the 47 wt% oxygen in the feedstock, Table 1).

3.2. Biomass pyrolysis

A duplicate red oak pyrolysis runs at 500 °C was performed in the fluidized bed reactor to generate bio-oil, char, and non-condensable gases. The overall mass balance closure (Table 5) for the liquid, solid, and gas were 86.2 and 85.5%, respectively, for the duplicate runs. The unknown masses might be attributed to bio-oil residue left in pipes and fittings and there was likely some error associated with measuring the non-condensable gases. Upon fast pyrolysis, the red oak was transformed into liquid bio-oil (61.1 wt%), char (11.6 wt%) and gases (13.2 wt%). In the bio-oil, a 26.8 wt% of water was present, which allowed the resulting bio-oil to flow. Among the non-condensable gases generated, carbon dioxide and carbon monoxide were predominant, supporting the importance of decarboxylation and decarbonylation for biomass deoxygenation during pyrolysis [22]. Sufficient reproduction of the process operating conditions (temperatures, feeding rate, vapor residence time, and

Table 4
Elemental analysis of the whole bio-oil.

	Run 1	Run 2	Average	STD	RSD
Carbon	57.5	61.3	59.4	1.9	3.1
Hydrogen	5.9	4.6	5.2	0.6	12.3
Oxygen	36.6	34.1	35.3	1.2	3.5

Numbers in the first two columns are in wt% based on whole bio-oil. Oxygen was calculated by difference.

Table 5
Overall mass balance for the pyrolysis runs.

	Run 1	Run 2	Average	STD
Bio-oil	61.90	60.33	61.11	0.79
Organics	45.36	44.02	44.69	-
Water	16.54	16.31	16.42	0.11
Char	11.30	11.86	11.58	0.28
Non-condensable gases	13.04	13.34	13.19	0.15
H_2	0.01	0.01	0.01	0.00
CH_4	0.50	0.47	0.48	0.01
C_2H_6	0.04	0.02	0.03	0.01
C_2H_4	0.16	0.17	0.16	0.01
CO	5.39	5.29	5.34	0.05
CO_2	6.94	7.38	7.16	0.22
Total	86.24	85.53	85.89	0.35

All numbers in wt% based on feedstock.

condensing rate) between runs was achieved such that the results were reproducible, which was indicated by the small standard deviation between the lumped products of the duplicate runs.

3.3. Bio-oil characterization

The whole bio-oil collected during the continuous run was separated into water-soluble and water-insoluble fractions by water extraction of the whole bio-oil. The resulting distribution for the whole bio-oil as shown in Table 6 demonstrated that water-soluble fraction constituted approximately 71 wt% of the whole bio-oil. The 29 wt% remainder, which was water-insoluble fraction, was close to the lignin content (33.3 wt%) in the original feedstock. This result was consistent with expectation as the bio-oil was the major product from fast pyrolysis and the lignin-derived product in the bio-oil was primarily pyrolytic lignin which would be hydrophobic.

Table 7 lists 50 compounds and additional groups of compounds present in at least 0.01 wt% that were identified and quantified by the integrated analytical techniques. The values shown are for the analysis of each of the water-soluble and water-insoluble fractions as well as the whole bio-oil. Statistical information for the duplicate runs is given in the fourth and fifth columns. Theoretical composition of whole bio-oil was calculated using yield of each of water-soluble and water-insoluble fractions and its distribution in the whole bio-oil (from Table 6) and was demonstrated in sixth column. For the whole bio-oil, actual yields were compared to theoretical values in the last column. The calculations were intended to show how precisely and accurately the pyrolysis experiments and chemical analyses were performed in the study. Although some sugars and pyrolytic lignin were not individually determined due to limitations of the analytical techniques, their amounts were found in lumped groups, which were also included in the overall mass balance.

3.3.1. Gas chromatography analysis of bio-oils

When the diluted bio-oil sample was injected into the GC system, only compounds volatile at 300 °C were able to pass through a capillary column to be separated, and detected by MS and FID. Forty major peaks were identified by the MS and quantified by the FID, contributing to approximately 25.3 wt% of the whole bio-oil. There is a potential to further improve the mass balance if comprehensive two-dimensional gas chromatography with its better separation of bio-oil species was used [23]. However, reasonable mass balances can be achieved even without using that more extensive approach. Expectedly, carbohydrate-derived compounds were predominant, constituting approximately 80% of the GC-detectables. For example, the weight percentages of glycolaldehyde, formaldehyde, methyl glyoxal, and acetol were 5.6, 3.5, 2.4, and 2.1 wt%, respectively, of the whole bio-oil. On the other hand, relatively small amounts of lignin-derived compounds were detected. Guaiacyl (G)- and syringyl (S)-type phenols were dominant over hydroxyl (H)-type phenol among the detected phenols, since hardwood lignin is mainly composed of G and S units [24]. In fact, nearly 95% of the GC-detectable phenols were hydroxyphenols with methoxy groups attached.

Table 6
Weight percentage for the water-soluble and water-insoluble fractions in the whole bio-oil.

	Run 1	Run 2	Average	STD
Water-solubles	69.9	71.2	70.5	0.6
Water-insolubles	30.1	28.8	29.4	–

The amount of the pyrolytic lignin measured was 16 wt%, which was lower than typically reported in the literature (25 wt%) [1], which was determined by the water extraction method of Meier et al. [18]. The lower value reported in the current work resulted from the method modification, which quantified some of the species in pyrolytic lignin thereby removing them from the lumped group. The quantification process in this study used an extra step to filter out water soluble compounds (phenol, sugars, and LMWs) still present in the water-insoluble fraction prior to injection into the GC. While the quantity of the remaining pyrolytic lignin after the extra extraction step was accurately obtained, its exact structure was still unknown. However, it is widely accepted that pyrolytic lignin is comprised of oligomers resulting from lignin-derived phenolic compounds, which was evidenced by GPC analysis as discussed below.

3.3.2. High-performance liquid chromatography analysis of bio-oils

Although GC has been the most powerful and popular analytical technique for bio-oil characterization, the technique is limited to detection of volatile compounds determined at a given injector temperature. As a consequence, a significant amount of semi-/nonvolatile species cannot be characterized, leading to a low bio-oil mass balance closure [8–10]. Additionally, the existence of high-molecular-weight compounds was supported by GPC analysis as presented in Table 8. For this study, an HPLC with two Bio-Rad Aminex HPX-87P columns was used to detect high-molecular-weight compounds in bio-oil, such as levoglucosan, cellobiosan, and maltosan. The total sugar estimated amount in bio-oil was determined with an HPLC with a HyperRez XP carbohydrate after acid-hydrolysis of bio-oil samples.

In the HPLC analysis, identification of a sugar was performed by comparing its peak retention time with that of each sugar in a standard mixture. Quantification of levoglucosan, which has been characterized by GC in many research groups [8–10,25], was instead determined using HPLC in the study since its boiling point is similar to the injector temperature that was employed for the GC analysis. The close alignment of temperature might lead to only partial volatilization of the levoglucosan and thus underestimation of its content in the bio-oil using typical GC methods. In fact, the measured levoglucosan yield increased approximately 30% when characterized by HPLC, compared to GC. Anhydrosugars derived from cellulose, 1,6-anhydro-β-D-glucopyranose (levoglucosan), 1,6-anhydro-α-D-maltose (maltosan), and 1,6-anhydro-β-D-cellobiose (cellobiosan) were detected as 5.0, 1.6, and 1.2 wt%, respectively. Notably, the yield of maltosan having an α(1→4) glycosidic linkage was appreciable, although cellulose is a polysaccharide consisting of glucose connected by β(1→4) glycosidic linkage. Houminer and Patai [26] claimed that formation of maltosan takes place by an inversion of C_1 in cellobiosan which is a result of a levoglucosan dimerization creating a β(1→4) glycosidic linkage. Yields of glucose, xylose, and sorbitol were summed to calculate total sugars in the bio-oil. It was estimated

Table 7
Product distributions of the the water-soluble and water-insoluble fractions and the whole bio-oil.

Compound	Run 1			Run 2			Average			Standard deviation			Theoretical	A/B
	WSF	WIF	Whole	WSF	WIF	Whole	WSF	WIF	Whole, A	WSF	WIF	Whole	Whole, B	
GC detectables	29.45	17.88	25.82	27.06	17.57	27.32	28.25	17.72	26.82	1.19	0.15	0.25	25.60	1.04
Formaldehyde	4.45	–	3.48	4.19	0.27	5.06	4.32	–	4.27	0.13	–	0.79	3.22	1.32
Glycolaldehyde	7.72	1.00	5.19	7.90	0.79	7.05	7.81	0.90	6.12	0.09	0.11	0.93	5.81	1.05
Methyl glyoxal	3.08	–	2.76	2.50	0.20	2.19	2.79	–	2.47	0.29	–	0.28	2.37	1.04
Acetol	2.89	0.51	2.29	2.27	0.51	1.91	2.58	0.51	2.10	0.31	0.00	0.19	1.98	1.06
3-Hydroxypropanal	1.09	0.34	0.80	1.10	0.33	0.77	1.09	0.33	0.79	0.01	0.00	0.02	0.87	0.91
Dimethoxytetrahydrofuran	0.29	0.17	0.16	0.35	0.12	0.11	0.32	0.14	0.14	0.03	0.03	0.02	0.27	0.52
2-Hydroxy-3-oxobutanal	1.05	0.40	0.87	1.03	0.37	0.91	1.04	0.38	0.89	0.01	0.01	0.02	0.85	1.04
Furfural	0.85	0.85	1.00	0.79	0.81	0.73	0.82	0.83	0.87	0.03	0.02	0.14	0.82	1.05
2-Furanmethanol	0.23	0.21	0.23	0.22	0.21	0.23	0.22	0.21	0.23	0.00	0.00	0.00	0.22	1.06
2-Methyl-2-cyclopenten-1-one	0.10	0.09	0.11	0.09	0.08	0.09	0.10	0.09	0.10	0.01	0.01	0.01	0.09	1.06
2-Hydroxy-2-cyclopenten-1-one	1.06	0.42	0.81	0.91	0.37	0.75	0.99	0.39	0.78	0.07	0.03	0.03	0.82	0.96
5-Methyl furfural	0.16	0.17	0.19	0.17	0.118	0.19	0.16	0.17	0.19	0.00	0.00	0.00	0.17	1.11
3-Methyl-2-cyclopenten-1-one	0.09	0.08	0.10	0.08	0.06	0.09	0.09	0.07	0.10	0.01	0.01	0.00	0.08	1.15
2(5*H*)-furanone	0.72	0.40	0.68	0.31	0.36	0.59	0.51	0.38	0.63	0.21	0.02	0.05	0.47	1.34
4-Hydroxy-5,6-dihydro-(2H)-pyran-2-one	1.14	0.51	1.00	1.40	0.59	1.11	1.27	0.55	1.05	0.13	0.04	0.06	1.06	0.99
Methylcyclopentenolone	0.41	0.35	0.40	0.32	0.29	0.30	0.37	0.32	0.35	0.05	0.03	0.05	0.35	1.00
Phenol	0.09	0.11	0.09	0.10	0.11	0.08	0.09	0.11	0.09	0.01	0.00	0.01	0.10	0.90
2-Methoxyphenol	0.13	0.12	0.19	0.15	0.28	0.07	0.14	0.20	0.13	0.01	0.08	0.06	0.16	0.82
2-Methoxy-4-methylphenol	0.04	0.25	0.10	0.06	0.26	0.09	0.05	0.25	0.09	0.01	0.00	0.00	0.11	0.85
4-Ethyl-2-methoxyphenol	0.18	0.13	0.14	0.15	0.13	0.16	0.17	0.13	0.15	0.02	0.00	0.01	0.15	0.98
2-Methoxy-4-vinylphenol	0.25	0.59	0.23	0.14	0.48	0.19	0.20	0.54	0.21	0.05	0.06	0.02	0.29	0.73
Eugenol	0.00	0.23	0.07	0.00	0.19	0.07	0.00	0.21	0.07	0.00	0.02	0.00	0.06	1.11
5-Hydroxymethyl furfural	0.65	0.24	0.40	0.38	0.24	0.37	0.51	0.24	0.38	0.13	0.00	0.02	0.43	0.88
2,6-Dimethoxyphenol	0.39	0.90	0.50	0.36	0.81	0.47	0.37	0.85	0.48	0.02	0.04	0.01	0.51	0.95
Isoeugenol	0.09	1.11	0.41	0.07	1.00	0.36	0.08	1.05	0.38	0.01	0.06	0.02	0.36	1.06
4-Methyl-2,6-dimethoxyphenol	0.25	0.77	0.41	0.23	0.85	0.38	0.24	0.81	0.40	0.01	0.04	0.01	0.41	0.97
Vanillin	0.15	0.26	0.17	0.10	0.25	0.15	0.12	0.25	0.16	0.03	0.01	0.01	0.16	0.99
4-Ethyl-2,6-dimethoxyphenol	0.08	0.34	0.14	0.07	0.35	0.08	0.08	0.34	0.11	0.00	0.00	0.03	0.15	0.74
4-Hydroxy-3-methoxyacetophenone	0.00	0.14	0.07	0.00	0.12	0.06	0.00	0.13	0.07	0.00	0.01	0.01	0.04	1.77
2,6-Dimethoxy-4-vinylphenol	0.15	1.07	0.43	0.16	1.19	0.43	0.16	1.13	0.43	0.00	0.06	0.00	0.44	0.98
4-Allyl-2,6-dimethoxyphenol	0.13	0.53	0.22	0.06	0.55	0.19	0.10	0.54	0.20	0.03	0.01	0.01	0.22	0.92
2,6-Dimethoxy-4-(1-propenyl)phenol	0.15	2.09	0.72	0.19	2.06	0.73	0.17	2.07	0.73	0.02	0.02	0.00	0.72	1.01
4-Hydroxy-3,5-dimethoxybenzaldehyde	0.26	0.57	0.26	0.17	0.52	0.22	0.21	0.54	0.24	0.05	0.03	0.02	0.31	0.78
4-Hydroxy-3,5-dimethoxyacetophenone	0.11	0.29	0.15	0.10	0.22	0.17	0.10	0.25	0.16	0.01	0.04	0.01	0.15	1.10
Sinapialdehyde	0.10	0.69	0.14	0.11	0.63	0.11	0.10	0.66	0.13	0.01	0.03	0.02	0.27	0.48
Levoglucosan-furanose	0.40	1.06	0.42	0.35	1.21	0.36	0.38	1.14	0.39	0.02	0.08	0.03	0.59	0.66
1,4-Benzenediol	0.15	0.08	0.13	0.12	0.18	0.10	0.13	0.13	0.11	0.02	0.05	0.02	0.13	0.86
1,4;3,6-Dihydro-α-D-glucopyranose	0.31	0.09	0.21	0.31	0.06	0.25	0.31	0.08	0.23	0.00	0.01	0.02	0.24	0.96
Methanol	–	0.34	0.10	–	0.39	0.11	–	0.36	0.10	–	0.03	0.00	0.11	0.91
Acetaldehyde	0.06	0.03	0.05	0.05	0.02	0.04	0.05	0.03	0.04	0.01	0.00	0.01	0.04	0.96
IC detectables	11.06	1.91	7.09	10.19	1.69	6.94	10.62	1.80	7.01	0.43	0.11	0.07	8.07	0.87
Acetic acid	7.75	1.37	5.28	7.11	1.30	5.38	7.43	1.33	5.33	0.32	0.04	0.05	5.66	0.94
Propanoic acid	0.36	0.04	0.21	0.28	0.06	0.11	0.32	0.05	0.16	0.04	0.01	0.05	0.25	0.65
Glycolic acid	1.71	0.26	0.79	1.59	0.11	0.50	1.65	0.19	0.64	0.06	0.07	0.14	1.23	0.53
Formic acid	1.24	0.24	0.81	1.21	0.22	0.95	1.22	0.23	0.88	0.01	0.01	0.07	0.93	0.94
HPLC detectables	21.73	1.69	14.44	21.92	2.23	15.86	21.82	1.96	15.14	0.09	0.27	0.71	15.41	0.98
Cellobiose	0.10	0.00	0.10	0.39	0.00	0.20	0.25	0.00	0.15	0.14	0.00	0.05	0.18	0.83
Cellobiosan	1.52	0.04	1.19	1.65	0.04	1.20	1.58	0.04	1.20	0.07	0.00	0.00	1.14	1.05
Xylose	1.22	0.05	0.91	1.22	0.05	0.90	1.22	0.05	0.90	0.00	0.00	0.00	0.88	1.03
Maltosan	2.37	0.16	1.69	2.23	0.16	1.66	2.30	0.16	1.67	0.07	0.00	0.02	1.68	1.00
Levoglucosan	8.12	0.43	5.14	6.60	0.43	4.92	7.36	0.43	5.03	0.76	0.00	0.11	5.35	0.94
Unidentified oligosaccharides	8.40	0.30	5.41	9.83	1.55	6.98	9.11	0.92	6.19	0.71	0.62	0.78	6.19	1.12
Karl-Fischer detectables	28.00	23.73	26.71	29.07	21.74	27.31	28.53	22.73	27.01	0.54	1.00	0.30	–	–
Water	28.00	23.73	26.71	29.07	21.74	27.31	28.53	22.73	27.37	0.54	1.00	0.66	–	–
Moisture water	–	–	13.49	–	–	13.84	–	–	13.66	–	–	0.18	–	–
Dehydration water	–	–	13.23	–	–	13.47	–	–	13.35	–	–	0.12	–	–
Others	–	54.39	16.35	–	56.82	15.76	–	55.60	16.07	–	1.21	0.28	–	–
Pyrolytic lignin	–	54.39	16.35	–	56.82	15.76	–	55.60	16.07	–	1.21	0.28	–	–
Total	90.24	–	90.41	88.24	–	93.19	89.24	–	91.80	1.00	–	1.39	–	–

All numbers in wt% based on each bio-oil.
WSF stands for water-soluble fraction of bio-oil.
WIF stands for water-insoluble fraction of bio-oil.
Whole stands for whole bio-oil.
Theoretical whole stands for calculated composition of the whole bio-oil, based on yields of water-soluble and water-insoluble fractions and its distribution in the whole bio-oil.
Unidentified oligosaccharides were quantified by a subtraction of characterized sugars from total sugars estimated by acid-hydrolysis technique.
Dehydration water was quantified by a subtraction of moisture water in feedstock from water content of the whole bio-oil (by Karl Fischer).

that around 15 wt% of the bio-oil consisted of sugars, including water-soluble sugars. Although approximately two-thirds of the feedstock was carbohydrates, only a small portion of the sugars were retained through fast pyrolysis, demonstrating a significant thermal degradation of the sugars during pyrolysis. Although a half of the quantified sugars by acid hydrolysis were not structurally identified in the study, it was speculated that the unidentified sugars were dimers of levoglucosan with glycosidic linkage of α or

Table 8
Molecular weight analysis of the whole bio-oil by GPC.

	M_w	M_n	M_w/M_n
Run 1	396	215	1.84
Run 2	388	214	1.81

M_w is the weight-average molecular weight and M_n is the number-average molecular weight.

β(1→2) and α or β(1→3), anhydrous dimers of xylose with all possible glycosidic linkages, or trimers/tetramers of the hexose and pentose. Those sugars were labeled as unidentified oligosaccharides in Table 7.

3.3.3. Ion chromatography analysis of bio-oils

Carboxylic acids as reported in Table 7 were characterized by IC rather than GC, due to their thermal instability and broad peak shape in the GC chromatograms. Whole bio-oil consisted of approximately 7 wt% organic acids including acetic, propanoic, glycolic, and formic acids. Along with glycolaldehyde, acetic acid was a major product of red oak pyrolysis, corresponding to over 5 wt% yield.

3.3.4. Gel permeation chromatography analysis of bio-oils

As determined by GPC, the weight-average molecular weights (M_w) for the whole bio-oils generated from the duplicate runs were 396 and 388, while the number-average molecular weights (M_n) were 215 and 214 (Table 8). The polydispersities (PD = M_w/M_n) for the bio-oils were 1.84 and 1.81, indicating a wide range of molecular weight distributions. It was noted that the weight-average molecular weight was higher than any identified/quantified compound in the bio-oils, such as levoglucosan (162.1), cellobiosan (324.3), and 4-allyl-2,6-dimethoxyphenol (194.2). This result suggested that the unidentified species (some sugars and pyrolytic lignin) in the bio-oil were mainly comprised of heavy molecules (dimers and trimers).

3.3.5. Product distributions of whole bio-oil, water-solubles, and water-insolubles

As shown in Table 7, the integration of analysis techniques led to a mass balance closure for the whole bio-oil of 92 wt%, with 27 wt% by Karl-Fischer titration, 26 wt% by GC, 15 wt% by HPLC, 7 wt% by IC, and 16 wt% pyrolytic lignin. Of the analytical techniques employed, GC as expected gave quantification for the largest organic portion of the bio-oil, but HPLC and IC, which have not been normally used for bio-oil characterization, accounted for an appreciable amount (22 wt%). With the concomitant quantification of the pyrolytic lignin, the remaining mass could be at least partially due to the presence of small unidentified peaks in the GC chromatograms. High mass closure as well as data reproducibility/accuracy as indicated by the low standard deviations and the values of A/B close to unity (Table 7) demonstrated successful and reliable pyrolysis experiments and chemical analyses of the collected bio-oil. As shown in Fig. 3, pyrolytic lignin (derived from lignin, 16 wt%), low-molecular-weight compounds, LMWs (derived from carbohydrates, 16 wt%) and sugars (derived from carbohydrates, 15 wt%) were the most predominant organic compounds in the whole bio-oil. Carboxylic acids, phenols, furans, cyclics represented smaller fraction of the whole bio-oil, making up 7, 4, 2, and 2 wt% of the whole bio-oil, respectively. It is noted that relatively large difference was observed between runs for LMWs, resulting from broad peak shapes of glycolaldehyde and formaldehyde on GC analysis.

Breakdowns of the water-soluble and water-insoluble fractions are shown in Figs. 4 and 5. The water-soluble fraction was about 70 wt% of whole bio-oil and mainly consisted of

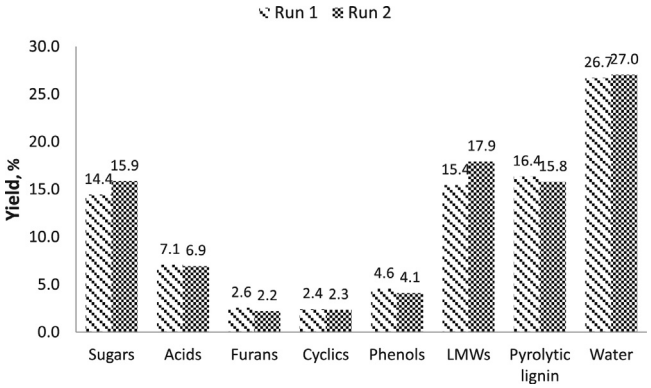

Fig. 3. Product distribution of whole bio-oil.

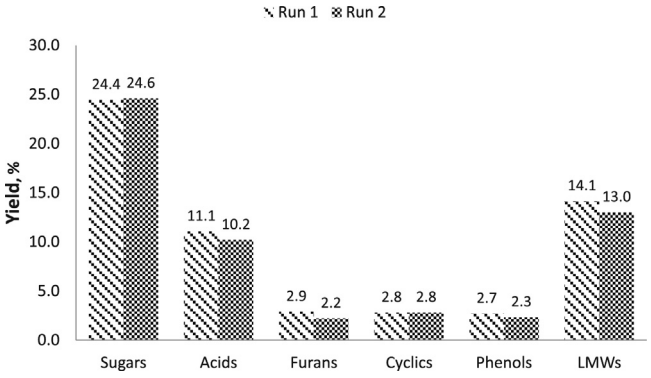

Fig. 4. Product distribution of water-soluble fraction.

carbohydrate-derived compounds such as sugars, LMWs, and acids. In the water-soluble fraction, there were small amounts of hydroxyphenols with two methoxy groups attached, such as 2,6-dimethoxyphenol and 4-methyl-2,6-dimethoxyphenol, derived from lignin. In contrast, a majority of the water-insolubles were lignin-derived compounds, including pyrolytic lignin (55.6 wt%) and phenols (10.4 wt%). The phenols present in the water-insolubles were mainly hydroxyphenols with one or two methoxy groups attached, such as 2,6-dimethoxy-4-(1-propenyl)phenol, 2,6-dimethoxy-4-vinylphenol, isoeugenol, 2,6-dimethoxyphenol, and 4-methyl-2,6-dimethoxyphenol. This speciation was likely due to hardwood lignin being composed of guaiacyl (with one methoxy group) and syringol (with two methoxy groups) units. Due to the difficulty in achieving completely clean phase separation, a small

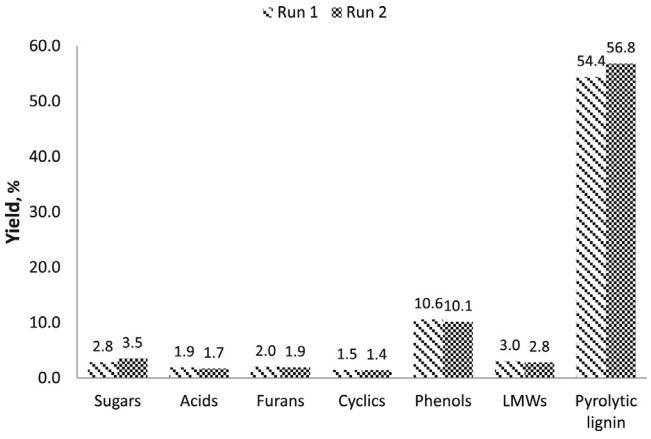

Fig. 5. Product distribution of water-insoluble fraction.

Table 9
Elemental balances throughout bio-oil, char, and non-condensable gases.

	Carbon	Hydrogen	Oxygen
Bio-oil (mol)	2.01	4.76	2.01
Char (mol)	0.73	0.45	0.15
Gas (mol)	0.40	0.16	0.52
Sum	3.14	5.36	2.67
Feedstock (mol)	3.82	6.68	2.96
Unaccounted (mol)	0.68	1.32	0.29
Unaccounted (wt%)	8.12	1.33	4.61

amount of water-soluble compounds such as sugars and acids was detected in the water-insoluble fraction.

3.4. Elemental balances throughout bio-oil, char, and gases

Elemental analysis of the whole bio-oil and char, and non-condensable gases product distributions were used to perform carbon, hydrogen, and oxygen balances on the pyrolysis products, which is shown in Table 9. Taking a basis of 100 g of red oak feedstock pyrolyzed, the overall balances on C, H, and O that could be accounted for in the balances from the pyrolysis products were 82.2, 80.2, and 90.2 wt%, respectively, 14.1 g of the feedstock was note directly unaccounted. Based on the elemental balances, the unaccounted mass would effectively have an empirical formula of $C_{2.3}H_{4.6}O$. The unaccounted mass could be attributed to bio-oil and char residues in the pipes and/or fittings which were not measured in the study. Of the C, H, and O, about 52% of the feedstock carbon was recovered in the form of bio-oil, primarily due to char production, whereas approximately 70 wt% of the hydrogen and oxygen in feedstock ended up in the bio-oil.

4. Conclusions

Bio-oils obtained from fast pyrolysis of red oak in a fluidized bed reactor were chemically analyzed using a broad range of analytical techniques. In contrast to the majority of pyrolysis studies that tend to focus only on the quantification of several key compounds (acetic acid, glycolaldehyde, and levoglucosan), 52 species were identified and quantified in the bio-oils, thereby achieving a high mass balance closure on the bio-oil of nearly 92 wt%. Duplicate pyrolysis runs demonstrated the high degree of data reproducibility. Although GC detectables occupied the largest portion of the organics in the bio-oil, the quantification of species by HPLC and IC appreciably contributed to the total mass balance closure. These results demonstrate the importance of using HPLC and IC to fully characterize bio-oil. The precise structure of all bio-oil products was not achieved as a significant portion (16 wt%) of the bio-oil was pyrolytic lignin and half of the quantified sugars appeared to be present in the form of dimers or oligomers, based on GPC analysis. While still not a complete compositional picture for the fast pyrolysis of biomass, this study provided the most complete analysis of composition while introducing complementary analytical techniques that refined the quantification. Understanding the true and detailed chemical composition of bio-oil as determined by the integrated analytical techniques in the study will be critical in identifying and solving problems that arise in optimizing downstream processes for upgrading the bio-oil into fuels and chemicals.

References

[1] D. Mohan, C.U. Pittman, P.H. Steele, Pyrolysis of wood/biomass for bio-oil: a critical review, Energy Fuels 20 (3) (2006) 848–889.
[2] C. Stevens, R.C. Brown, Thermochemical Processing of Biomass: Conversion into Fuels, Chemicals and Power, Vol. 12, Wiley, 2011.
[3] C.A. Mullen, A.A. Boateng, Chemical composition of bio-oils produced by fast pyrolysis of two energy crops†, Energy Fuels 22 (3) (2008) 2104–2109.
[4] J.P. Diebold, A review of the chemical and physical mechanisms of the storage stability of fast pyrolysis bio-oils 2000, National Renewable Energy Laboratory Golden, CO.
[5] G.W. Huber, S. Iborra, A. Corma, Synthesis of transportation fuels from biomass: chemistry, catalysts, and engineering, Chem. Rev. 106 (9) (2006) 4044–4098.
[6] G.W. Huber, et al., Production of liquid alkanes by aqueous-phase processing of biomass-derived carbohydrates, Science 308 (2005) 1446–2079.
[7] A.K. Sarma, D. Konwer, P. Bordoloi, A Comprehensive analysis of fuel properties of biodiesel from Koroch seed oil, Energy Fuels 19 (2) (2005) 656–657.
[8] L. Ingram, et al., Pyrolysis of wood and bark in an auger reactor: physical properties and chemical analysis of the produced bio-oils, Energy Fuels 22 (1) (2007) 614–625.
[9] C.U. Pittman Jr., et al., Characterization of bio-oils produced from fast pyrolysis of corn stalks in an auger reactor, Energy Fuels 26 (6) (2012) 3816–3825.
[10] C. Branca, P. Giudicianni, C. Di Blasi, GC/MS characterization of liquids generated from low-temperature pyrolysis of wood, Ind. Eng. Chem. Res. 42 (14) (2003) 3190–3202.
[11] D. Kunii, O. Levenspiel, Fluidization Engineering, Vol. 2, Butterworth-Heinemann, Boston, 1991.
[12] O. Faix, et al., Thermal degradation products of wood: gas chromatographic separation and mass spectrometric characterization of polysaccharide derived products, Holz als Roh-und Werkstoff 49 (5) (1991) 213–219.
[13] O. Faix, D. Meier, I. Fortmann, Thermal degradation products of wood. Gas chromatographic separation and mass spectrometric characterization of monomeric lignin-derived products, Holz als Roh-und Werkstoff 48 (7–8) (1990) 281–285.
[14] P.R. Patwardhan, R.C. Brown, B.H. Shanks, Understanding the fast pyrolysis of lignin, ChemSusChem 4 (11) (2011) 1629–1636.
[15] P.R. Patwardhan, et al., Product distribution from fast pyrolysis of glucose-based carbohydrates, J. Anal. Appl. Pyrol. 86 (2) (2009) 323–330.
[16] P.R. Patwardhan, R.C. Brown, B.H. Shanks, Product distribution from the fast pyrolysis of hemicellulose, ChemSusChem 4 (5) (2011) 636–643.
[17] Y. Huang, Q. Ou, W. Yu, Characteristics of flame ionization detection for the quantitative analysis of complex organic mixtures, Anal. Chem. 62 (18) (1990) 2063–2064.
[18] B. Scholze, D. Meier, Characterization of the water-insoluble fraction from pyrolysis oil (pyrolytic lignin). Part I. PY–GC/MS, FTIR, and functional groups, J. Anal. Appl. Pyrol. 60 (1) (2001) 41–54.
[19] S. Helle, et al., A kinetic model for production of glucose by hydrolysis of levoglucosan and cellobiosan from pyrolysis oil, Carbohydr. Res. 342 (16) (2007) 2365–2370.
[20] J. Lian, et al., Separation: hydrolysis and fermentation of pyrolytic sugars to produce ethanol and lipids, Bioresource Technol. 101 (24) (2010) 9688–9699.
[21] A. Demirbaş, Calculation of higher heating values of biomass fuels, Fuel 76 (5) (1997) 431–434.
[22] M. Zabeti, et al., In situ catalytic pyrolysis of lignocellulose using alkali-modified amorphous silica alumina, Bioresource Technol. 118 (2012) 374–381.
[23] J. Marsman, et al., Identification of components in fast pyrolysis oil and upgraded products by comprehensive two-dimensional gas chromatography and flame ionisation detection, J. Chromatogr. A 1150 (1) (2007) 21–27.
[24] B.M. Dolgonosov, T.N. Gubernatorova, Modeling the biodegradation of multicomponent organic matter in an aquatic environment: 2. Analysis of the structural organization of lignin, Water Resources 37 (3) (2010) 320–331.
[25] P.R. Patwardhan, et al., Distinguishing primary and secondary reactions of cellulose pyrolysis, Bioresource Technol. 102 (8) (2011) 5265–5269.
[26] Y. Houminer, S. Patai, Thermal polymerization of levoglucosan, J. Polym. Sci. Part A-1: Polym. Chem. 7 (10) (1969) 3005–3014.